

Università degli Studi di Napoli “Federico II”



**SCUOLA POLITECNICA E DELLE SCIENZE DI BASE
DIPARTIMENTO DI INGEGNERIA INDUSTRIALE**

**CORSO DI LAUREA IN INGEGNERIA AEROSPAZIALE
CLASSE DELLE LAUREE IN INGEGNERIA INDUSTRIALE (L-9)**

Elaborato di laurea in Meccanica del Volo
**Evaluation of the downwash gradient on a 19-pax
aircraft model**

**Relatore:
Prof. Danilo Ciliberti**

**Candidato:
Leonardo Zolli
Matr. N35003665**

ANNO ACCADEMICO 2023 – 2024

Abstract

The downwash gradient at tailplane is a crucial parameter in the evaluation of the stability characteristics while developing a new aircraft: this work aims to evaluate the downwash gradient of the PROSIB pax 19 aircraft model by using 4 different methods, two of which can be implemented by simply applying a semi empiric formula (Prandtl and USAF DATCOM), while the other two need an analysis that will be done by VSPAERO, a linear solver that uses VLM (Vortex Lattice Methods) to simulate the flow field around an aircraft model generated in OpenVSP.

These calculations will be executed in six different conditions, varying the extension of the flaps from 0 to 30 degrees, with and without the propellers installed.

Sommario

Il gradiente di downwash è un parametro cruciale nella valutazione delle caratteristiche di stabilità durante la progettazione di un aeromobile: questo elaborato si pone l'obiettivo di valutare il gradiente di downwash del modello PROSIB pax 19 utilizzando 4 metodi diversi, due dei quali possono essere implementati semplicemente applicando una formula semi empirica (Prandtl e USAF DATCOM), mentre gli altri due richiedono un'analisi che sarà effettuata tramite VSPAERO, un risolutore numerico in grado di simulare il campo di flusso intorno ad un modello di aeromobile generato con OpenVSP.

Questi calcoli verranno eseguiti in sei diverse condizioni, variando l'estensione dei flaps da 0 a 30 gradi, con e senza i motori installati.

Table of contents

1. Introduction	4
1.1 Objectives	4
1.2 Layout of the work	4
2. Theoretical Background	5
2.1 Downwash angle	5
2.1.1 Contribution of flaps deflection.....	6
2.2 Downwash gradient contribution to stability and control	6
3. Software implementation	7
3.1 OpenVSP	7
3.2 VSPAERO	7
4. Results and discussion.....	9
4.1 Method A: Prandtl formula.....	9
4.2 Method B: DATCOM formula	11
4.3 Method C	14
4.2 Method D.....	27
5. Conclusion.....	32

List of figures

Figure 1 - Wing trailing vortex system.....	5
Figure 2 - OpenVSP main screen	7
Figure 3 - VSPAERO panel	8
Figure 4 - PROSIB 19 pax model with dimensions in mm	10
Figure 5 - KAR as a function of AR.....	12
Figure 6 - K lambda as a function of lambda	12
Figure 7 - KH as a function of lh and bh	13
Figure 8 - VSPAERO settings	15

Figure 9 - polar file copied on MS Excel	15
Figure 10 - CM wing-body-horizontal flaps 0 engines off.....	16
Figure 11 - CM wing-body, flaps 0 engines off	16
Figure 12 - CM body horizontal, flaps 0 engines off	17
Figure 13 - CM body, flaps 0 engines off	17
Figure 14 - CM wing-body-horizontal, flaps 0 engines on	18
Figure 15 - CM wing-body, flaps 0 engines on.....	19
Figure 16 - CM body-horizontal, flaps 0 engines on.....	19
Figure 17 - CM body-wing-horizontal, flaps 15 engines off.....	21
Figure 18 - CM wing-body, flaps 15 engines off	21
Figure 19 - CM wing-body-horizontal, flaps 15 engines on	22
Figure 20 - CM wing-body, flaps 15 engines on.....	23
Figure 21 - CM wing-body-horizontal, flaps 30 engines off.....	24
Figure 22 - CM wing-body, flaps 30 engines off	24
Figure 23 - CM wing-body-horizontal, flaps 30 engines on	25
Figure 24 - CM wing-body, flaps 30 engines on.....	26
Figure 25 - Method C table with VSPAERO data.....	27
Figure 26 - Stability curves for method D, flaps 0 engines off	28
Figure 27 - MS Excel command to find the angle of attack.....	28
Figure 28 - Epsilon vs alpha.....	29
Figure 29 - Stability curves for method D, flaps 0 engines on.....	30
Figure 30 - epsilon vs alpha, flaps 0 engines on.....	30

1. Introduction

1.1 Objectives

The objective of this thesis is to make an evaluation of the downwash gradient of the PROSIB pax 19 aircraft. This will be done by comparing the results of 4 different methods in 6 different conditions (with flaps at 0, 30 and 60 degrees, each considered both with and without propellers installed under the wing).

The first two methods consist in the application of the Prandtl formula and the USAF DATCOM formula. They will be applied only with flaps at 0° and without the propellers installed, as the influence of the deflection of the flaps and the presence of the propellers under the wing do not affect these two methods.

The third method consists of the comparison of the evaluation of the downwash gradient seen as a combination of the CM_α calculated for the whole aircraft and for the wing-body body-horizontal tail configuration and the fuselage alone. In this method, the presence of the vertical tail does not influence the simulation as the effect on the flow of the vertical tail is symmetrical on the lateral directional plane, therefore it can be neglected to make the simulation more computationally efficient.

The fourth and last method consists of the interpolation of the stability curve calculated with the tail removed with the one calculated with different values of the tail incidence angle, obtaining an epsilon vs AoA slope, from which we can obtain the downwash gradient.

1.2 Layout of the work

Chapter 2: This chapter contains all the preliminary considerations on the downwash angle, the downwash gradient and its influence on the stability of an aircraft.

Chapter 3: This chapter gives an overview of OpenVSP and VSPAERO and their main functionalities.

Chapter 4: This chapter describes in detail the four methods used in this evaluation and exposes the results obtained.

Chapter 5: This chapter compares the accuracy of the different methods with respect to the wind tunnel results.

2. Theoretical Background

2.1 Downwash angle

When considering a 2-dimensional airfoil, lift can easily be derived from the *Kutta – Joukowski Theorem*:

$$L = \rho V_{\infty} \wedge \Gamma \quad (2.1)$$

In a finite wing, the difference in pressure between the dorsal and ventral side of the wing generates a system of free vortices.

By looking at Figure 1, it is possible to see how these vortices tend to push the air downwards (downwash effect) for $-b/2 < y < b/2$, while the air is pushed upwards (upwash) for $y > b/2$ and $y < -b/2$

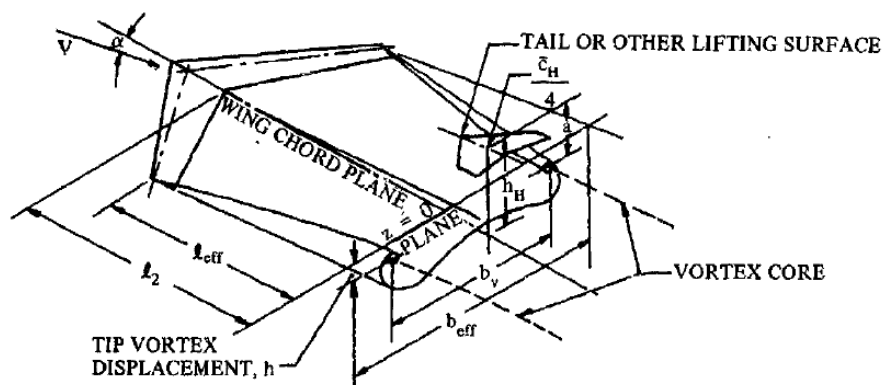


Figure 1 - Wing trailing vortex system

Mathematically, the downwash can be seen as a function of point P(x, y, z) in the flow field around the aircraft:

$$\varepsilon(x, y, z) = \tan^{-1} \frac{w(x,y,z)}{|u(x,y,z)|} \approx \frac{w(x,y,z)}{V_\infty} \quad (2.2)$$

2.1.1 Contribution of flaps deflection

The deflection of the flaps causes an increase in the spanwise loading on the wing, which increases the strength of the wing trailing vortex system, thus increasing the downwash gradient.

2.2 Downwash gradient contribution to stability and control

The downwash gradient has a very important role in determining the longitudinal stability of an aircraft.

The overall lift coefficient of an airplane is given by

$$C_L = \left(a_{wb} + \eta_H \frac{S_H}{S} \left(1 - \frac{d\varepsilon}{d\alpha} \right) a_H \right) \alpha \quad (2.3)$$

Where a_{wb} is the lift-curve slope for the wing-body combination and η_H is the ratio of the dynamic pressure acting on the horizontal tail to that relative to the wings.

In steady flight, the pitching moment coefficient is given by:

$$C_m = C_{m_0} + C_{m_\alpha} \alpha + C_{m_\delta} \delta \quad (2.4)$$

Where δ is the elevator deflection angle and

$$C_{m_0} = C_{m_{ac_{wb}}} + \eta_H V_H a_H (i_H + \varepsilon_0) \left[1 - \eta_H \frac{a_H S_H}{a S} \left(1 - \frac{d\varepsilon}{d\alpha} \right) \right] \quad (2.5)$$

Equations (2.3) - (2.5) highlight the influence of the downwash gradient $\frac{d\varepsilon}{d\alpha}$ on the longitudinal stability of an aircraft.

3. Software implementation

3.1 OpenVSP

OpenVSP (Open Vehicle Sketchpad) is an open-source parametric aircraft geometry software that allows to model an aircraft in order to test it with a number of structural and fluid dynamics tools.

The main screen consists of a visual editor that allows the user to model his aircraft into different elements as seen in Figure 2:

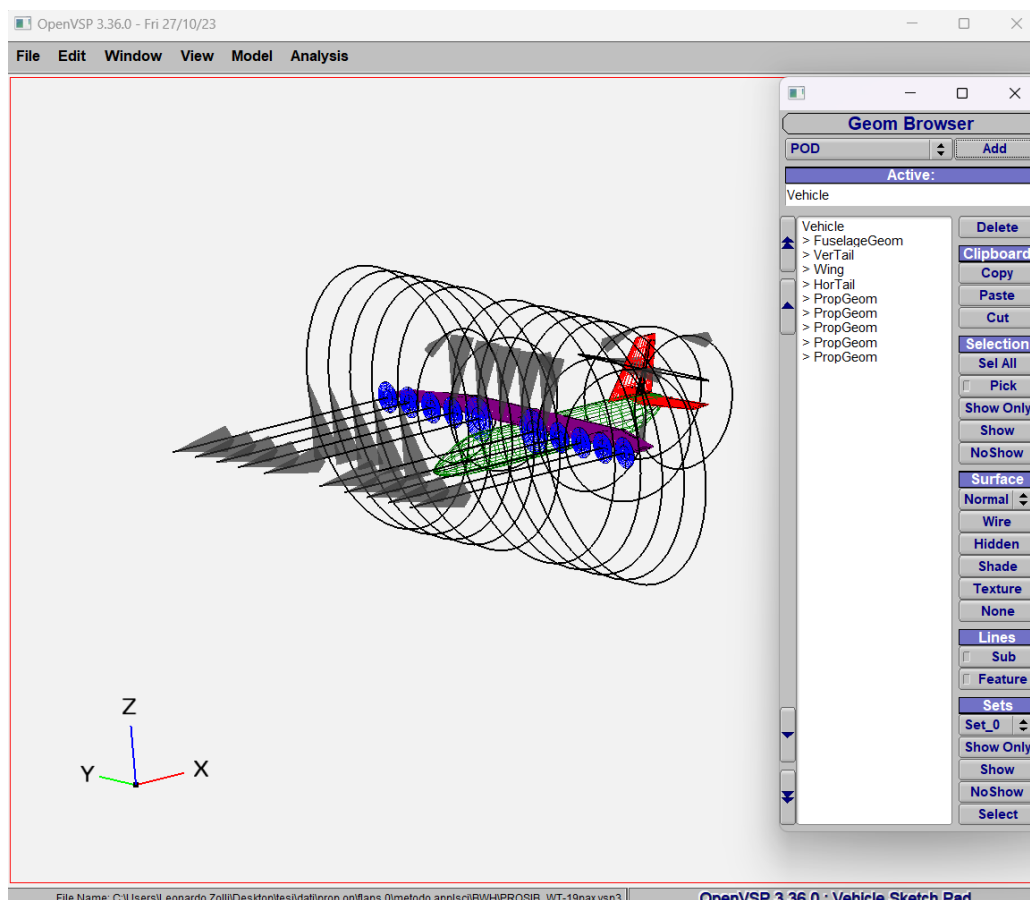


Figure 2 - OpenVSP main screen

3.2 VSPAERO

VSPAERO is a fast, linear solver that applies discrete vortices to each panel generated by OpenVSP degengeom file in order to evaluate the pressure distribution around the model.

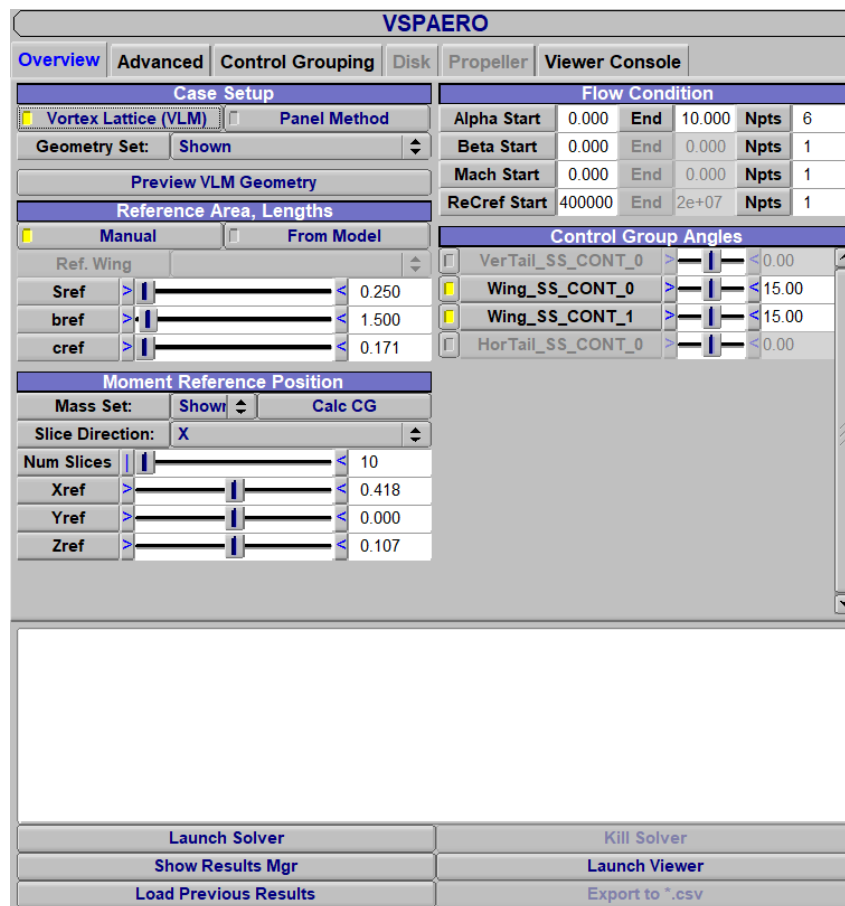


Figure 3 - VSPAERO panel

The VSPAERO visual interface allows the user to adjust all the settings such as the flow conditions and the control surfaces before running the simulation.

After the simulation has been executed, a series of files will be generated containing all the information gathered during the analysis.

For the purposes of this work, it is of particular interest to focus on the .polar file, which will contain a table that displays all the coefficients relevant to an aerodynamic analysis calculated for each angle of attack that has been specified in the “Flow condition” section of the VSPAERO settings.

4. Results and discussion

4.1 Method A: Prandtl formula

The first method to determine the downwash gradient is applied by using the following formula attributed to Prandtl:

$$\left(\frac{d\varepsilon}{d\alpha}\right)_H \approx \left(\frac{d\varepsilon}{d\alpha}\right)_\infty = 2 \frac{C_{L\alpha,W}}{\pi AR e_w} \quad (4.1)$$

where:

- $\left(\frac{d\varepsilon}{d\alpha}\right)_H$ is the downwash gradient at tailplane
- $\left(\frac{d\varepsilon}{d\alpha}\right)_\infty$ is the downwash gradient at far downstream
- $C_{L\alpha,W}$ is the derivative of the lift coefficient in the angle of attack considered at the wing
- AR is the aspect ratio of the wing
- e_w is the efficiency factor of the wing

All the geometric variables needed in Equation 4.1 can be obtained from Figure 4, while the value of $C_{L\alpha,W}$ comes from the Polhamus Formula

$$C_{L\alpha} = \frac{2\pi AR}{2 + \sqrt{4 + \frac{AR^2(1-M_\infty^2)}{k_p^2} \left(1 + \frac{\tan^2 \Lambda_c/2}{1-M_\infty^2}\right)}} \quad (4.2)$$

$$\text{where } k_p = \begin{cases} 1 + AR \frac{1.87 - 0.000233\Lambda_{le}}{100}, & x < 0 \\ 1 + \frac{(8.2 - 2.3\Lambda_{le}) - AR(0.22 - 0.153\Lambda_{le})}{100}, & x \geq 0 \end{cases}$$

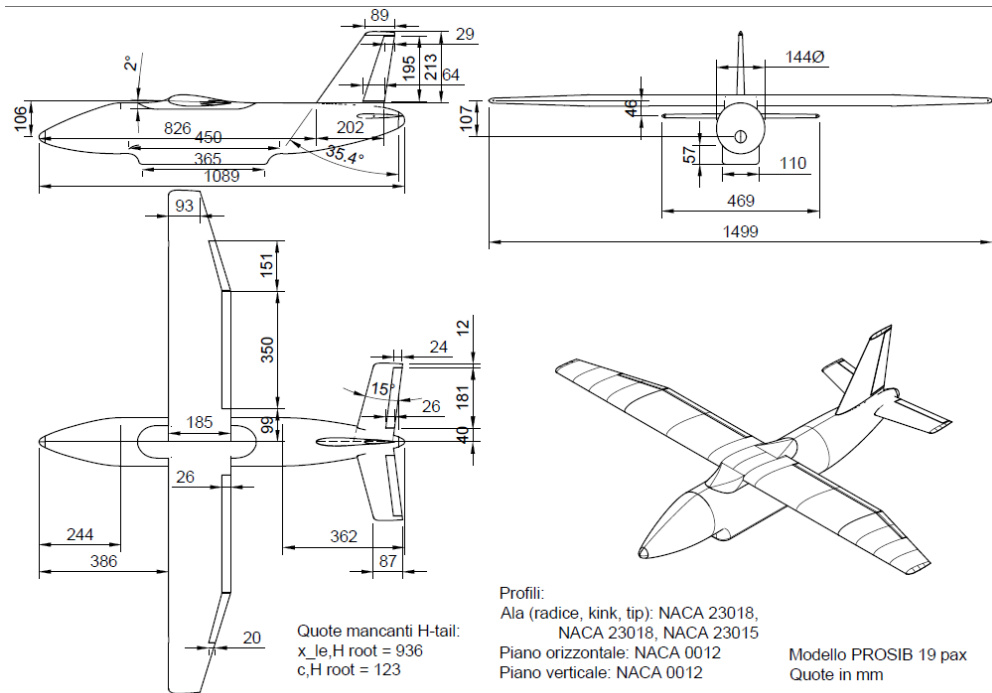


Figure 4 - PROSIB 19 pax model with dimensions in mm

By using the data coming from Figure 4 - PROSIB 19 pax model with dimensions in mm and putting them into equation 4.2 we are able to obtain all the variables needed to evaluate the downwash gradient using equation 4.1:

Item	Symbol	Value
Lift coefficient	$C_{L\alpha}$	5.28
Aspect Ratio	AR	9
Efficiency factor	e_w	0.9

Table 1

Therefore, we get the desired value of the downwash gradient:

$$\left(\frac{d\varepsilon}{d\alpha}\right)_H = 0.415$$

4.2 Method B: DATCOM formula

The same number can be evaluated more accurately by using Equation 4.3, a formula presented in the *USAF Stability and Control DATCOM*, a collection of knowledge, opinions and judgment in the area of aerodynamic stability and control prediction methods.

$$\left(\frac{d\varepsilon}{d\alpha}\right)_H = 4.44 \sqrt{1 - M_\infty^2} (K_{AR} K_\lambda K_H \sqrt{\cos \Lambda_{c/4W}})^{1.19} \quad (4.3)$$

K_{AR} , K_λ and K_H are coefficient that can be derived as it follows:

$$K_{AR} = \frac{1}{AR} - \frac{1}{1 + AR^{1.7}} \quad (4.4)$$

$$K_\lambda = \frac{10 - 3\lambda}{7} \quad (4.5)$$

$$K_H = \frac{1 - \left|\frac{h_H}{b}\right|}{\sqrt{\frac{2l_H}{b}}} \quad (4.6)$$

Where:

- **AR** is the aspect ratio of the wing
- **b** is the wingspan
- **λ** is the taper ratio
- **h_H** and **l_H** are the coordinates of the horizontal tail aerodynamic center with respect to the wing aerodynamic center.

Figures 5 to 7 show a plot of each of those coefficients varying in function of their parameters:

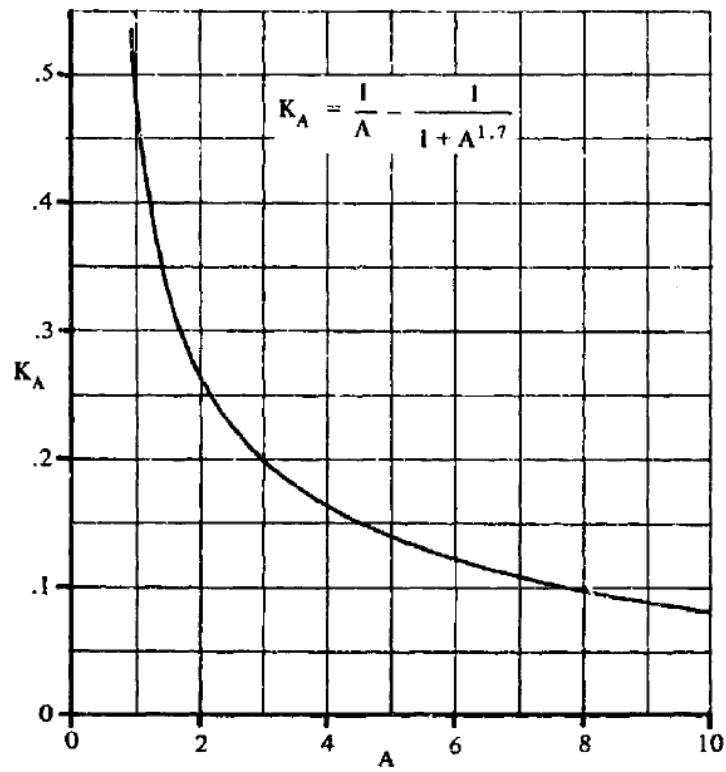


Figure 5 - K_A as a function of A

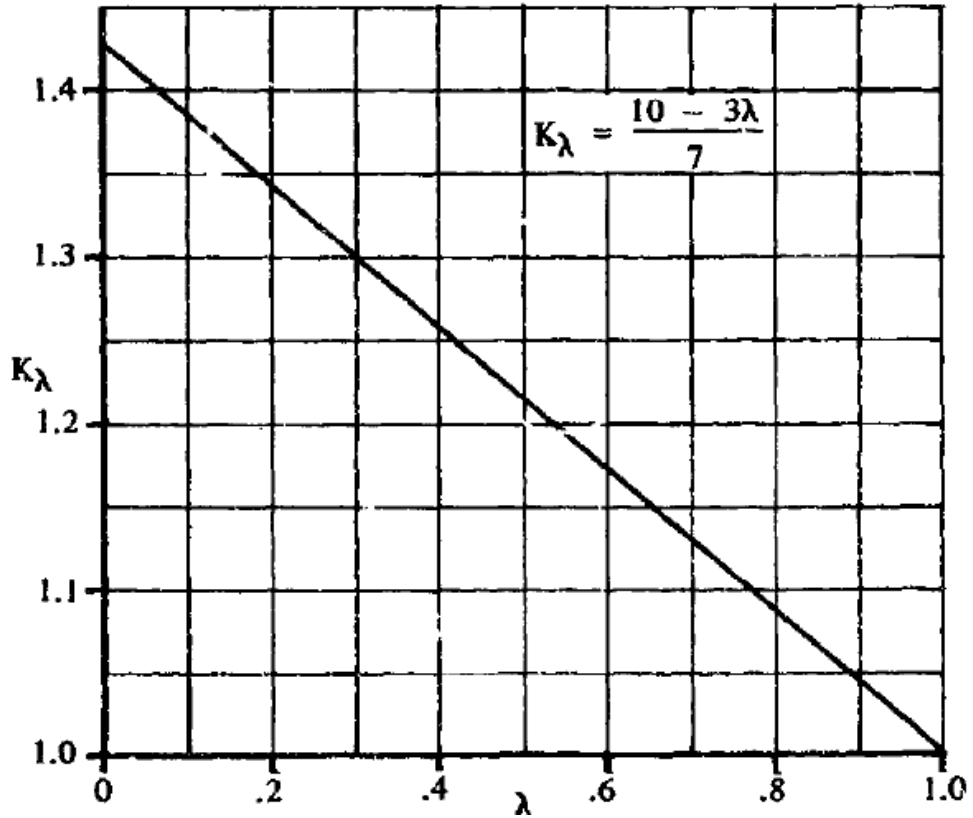


Figure 6 - K_λ as a function of λ

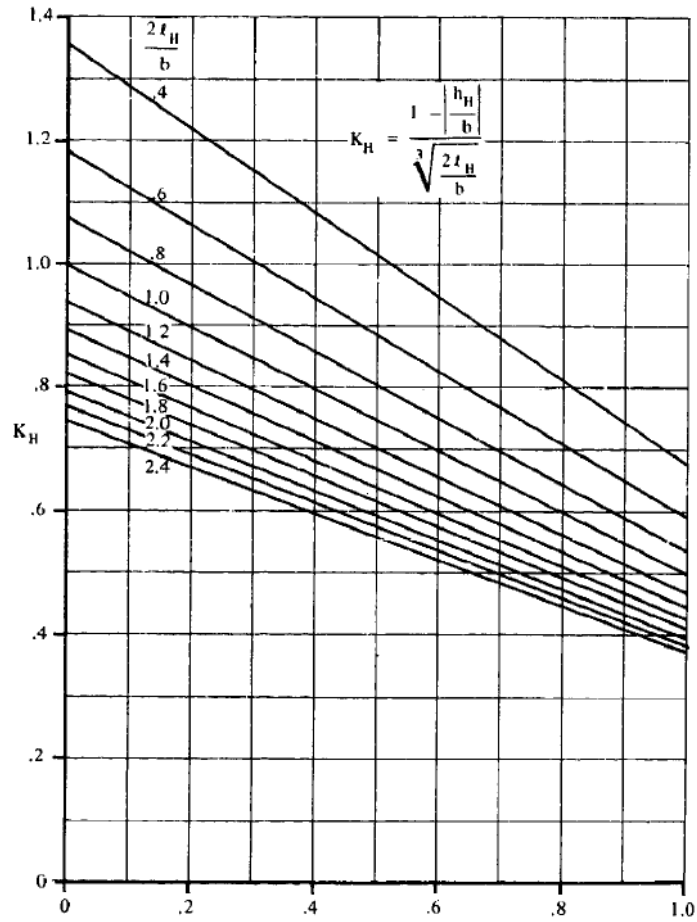


Figure 7 - K_H as a function of lh and bh

Once again, it is possible to derive all the coefficients needed from Figure 4:

Coefficient	Value
K_{AR}	0.088
K_λ	1.213
K_H	1.084

Table 2

Considering negligible the value of $\Lambda_{c/4,W}$, as the wing is straight and untapered, we get to the final result of the downwash gradient with the DATCOM method:

$$\left(\frac{d\varepsilon}{d\alpha}\right)_H = 0.340$$

4.3 Method C

In this case we will have to evaluate the downwash gradient at different inclinations of the flaps and considered both the prop off and prop on configurations, as these do have an influence on the final value.

This method consists of running 4 simulations using OpenVSP to gather the value of $C_{L\alpha}$ in a wing-body, wing-horizontal, body and complete configuration of the aircraft and of finally combining them in Equation 4.4

$$1 - \frac{d\varepsilon}{d\alpha} \approx \frac{C_{M\alpha,WBH} - C_{M\alpha,WB}}{C_{M\alpha,BH} - C_{M\alpha,B}} \quad (4.7)$$

In this work, this method will be applied to determine the downwash gradient in 3 different flaps configurations.

In order to obtain the value of $C_{M\alpha,WBH}$, a VSPAERO simulation has to be made after giving the solver the settings shown in Figure 8:

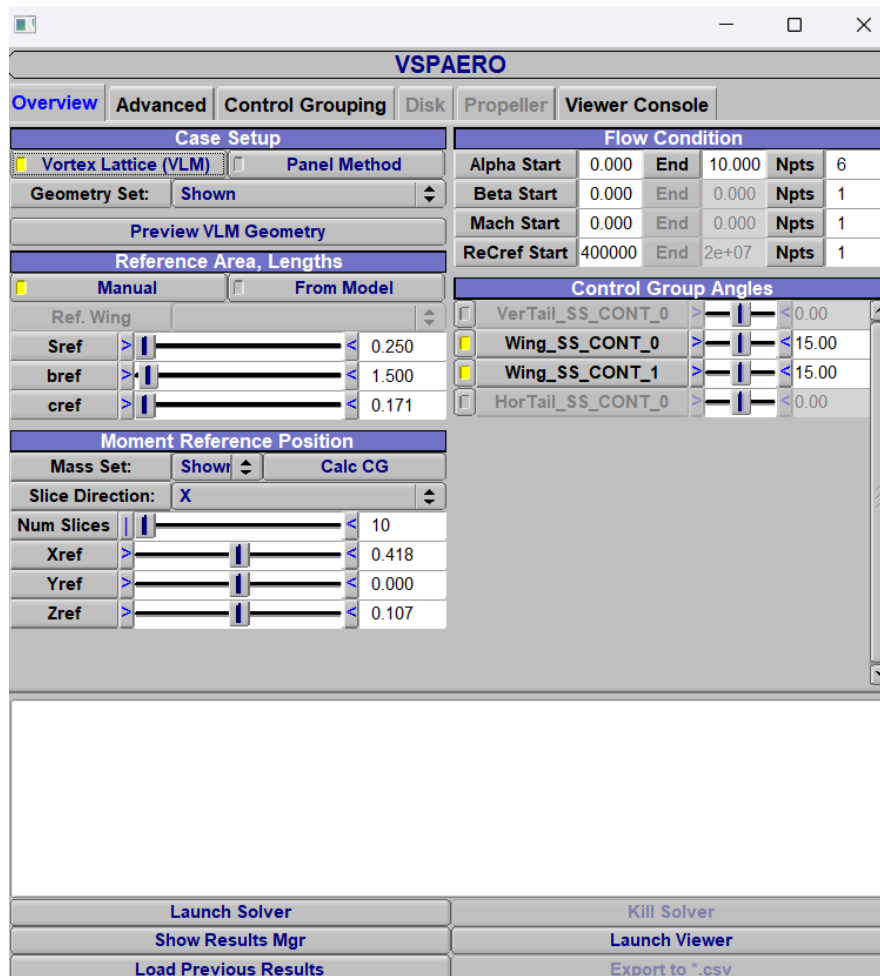


Figure 8 - VSPAERO settings

After the simulation has been executed, a .polar file containing all the useful data is automatically generated and can be extracted and copied in a spreadsheet.

In this work, Microsoft Excel will be used to manage all the data coming from VSPAERO.

Beta	Mach	AoA	Re/1e6	CL	CD0	CDi	CDtot	CDt	CDtot_t	CS	L/D	E	CFx	CFy	CFz	CMx	CMy	CMz	CMI	CMi	
0	0	0	0	0.4	0.089888	0.013783	0.000333	0.014117	0.000295	0.014078	2.39E-06	6.367551	0.020243	0.014117	2.39E-06	0.089888	6.66E-06	-0.02169	9.65E-07	-6.7E-06	-0.
0	0	2	0.4	0.254768	0.014154	0.002614	0.016768	0.002513	0.016667	3E-06	15.19397	0.136907	0.007866	3E-06	0.255198	-1.6E-05	-0.01135	-1.4E-06	1.65E-05	-0.	
0	0	4	0.4	0.419521	0.014831	0.007043	0.021874	0.006906	0.021737	4.8E-06	19.17856	0.284562	-0.00744	4.8E-06	0.420025	8.48E-05	0.000647	8.92E-06	-8.5E-05	0.0	
0	0	6	0.4	0.583145	0.015802	0.013564	0.029366	0.013179	0.02898	2.37E-05	19.85788	0.40956	-0.03175	2.37E-05	0.58302	0.000129	0.014249	2.11E-05	-0.00013	0.0	
0	0	8	0.4	0.746046	0.017056	0.022141	0.039197	0.019498	0.036555	-1.9E-05	19.0332	0.50221	-0.06501	-1.9E-05	0.744241	0.000151	0.02938	1.01E-05	-0.00015	0.	
0	0	10	0.4	0.907669	0.018574	0.032737	0.051311	0.028823	0.047397	-5.2E-05	17.68942	0.56787	-0.10708	-5.2E-05	0.90279	0.000215	0.046097	1.47E-05	-0.00022	0.0	
				0.081805	CLa												0.006782	CMa			

Figure 9 - polar file copied on MS Excel

As shown in Figure 8, the SLOPE() command allows us to obtain a value of $C_{M\alpha, WBH}$, and a plot of C_M against the angle of attack α can be easily generated and is shown in Figure 10.

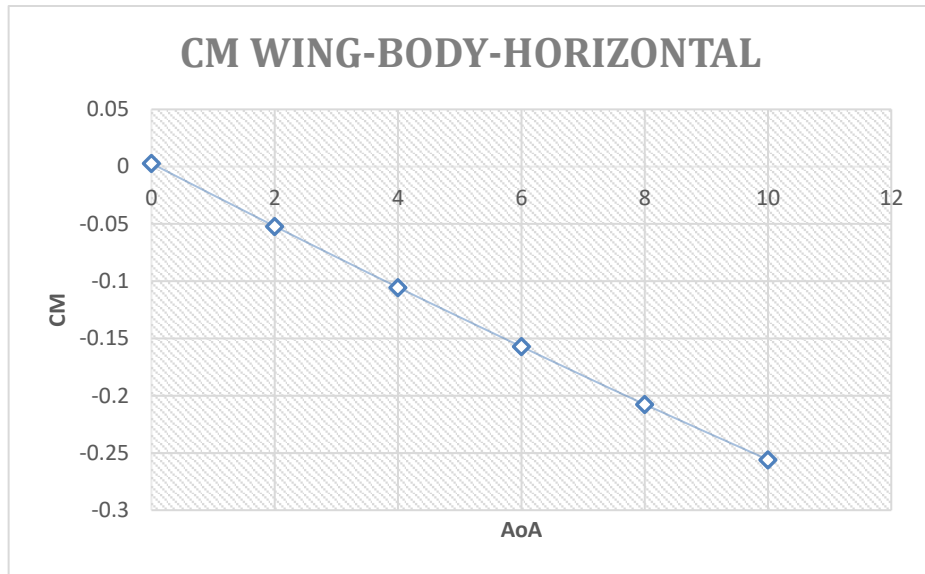


Figure 10 - CM wing-body-horizontal flaps 0 engines off

The following figures illustrate the C_M vs α plot of the other configurations, that are body – wing, body – horizontal and body, while Table 3 summarizes the value of $C_{M\alpha}$ for all four configurations.

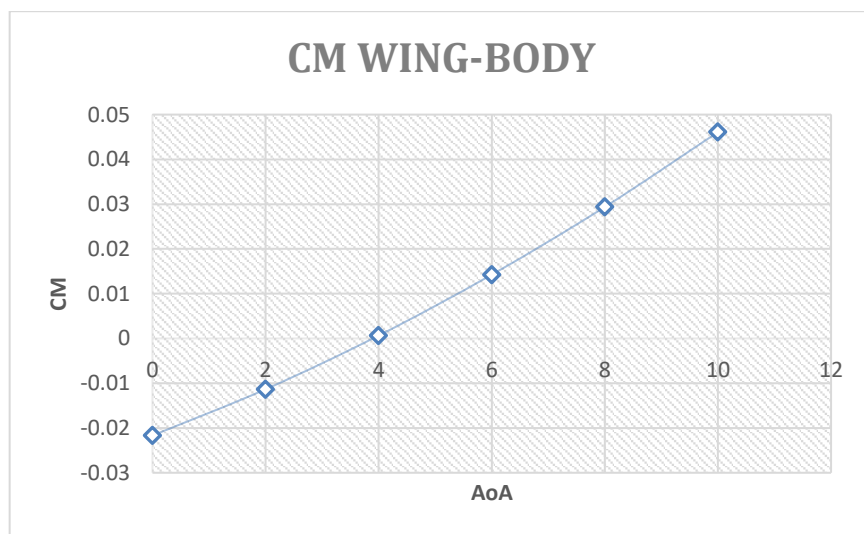


Figure 11 - CM wing-body, flaps 0 engines off

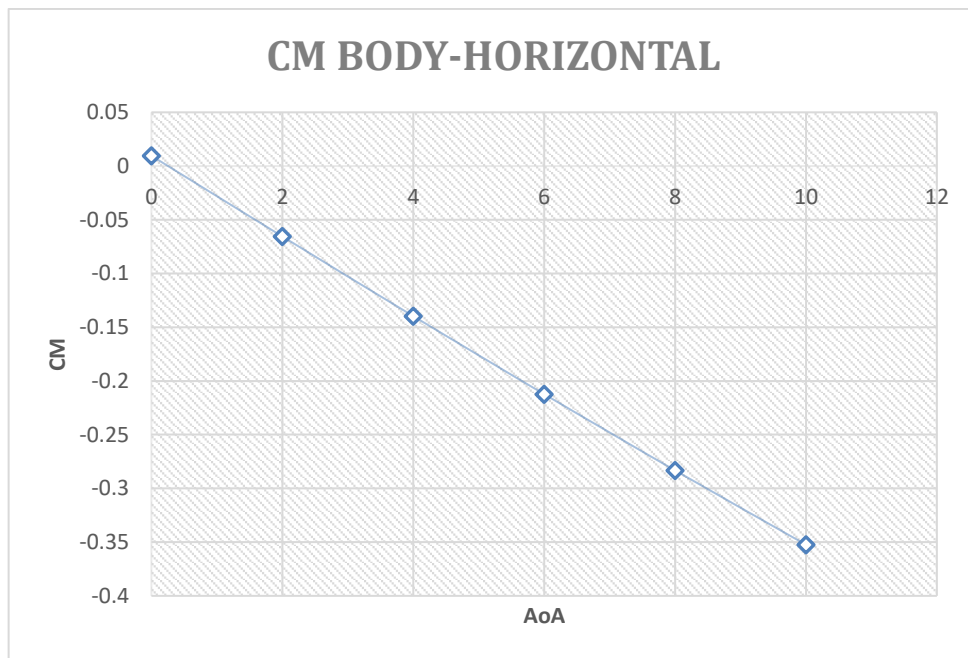


Figure 12 - CM body horizontal, flaps 0 engines off

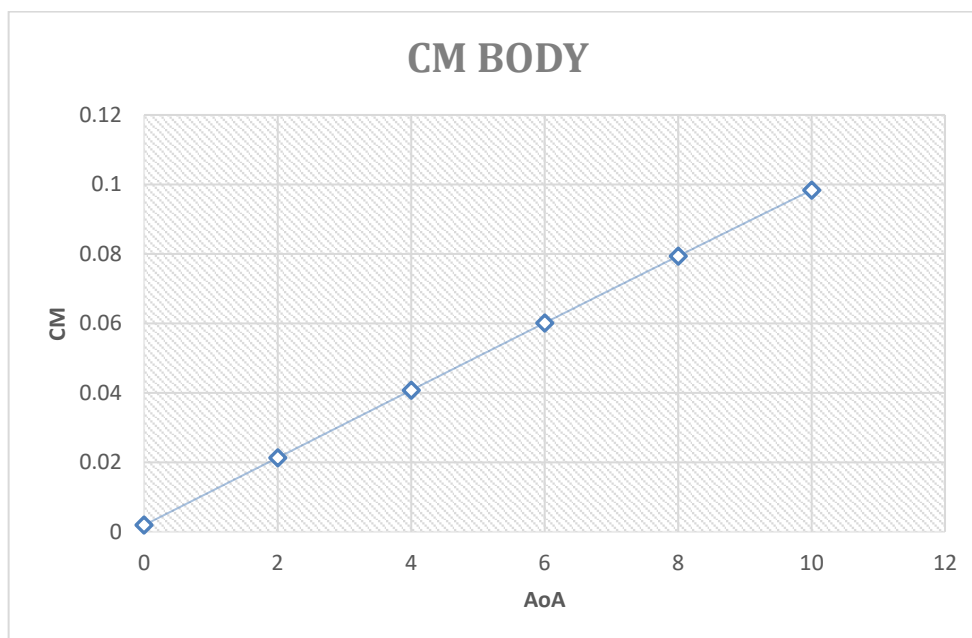


Figure 13 - CM body, flaps 0 engines off

Configuration	$C_{M\alpha}$
BWH	-0.026
BW	0.007
BH	-0.036
B	0.010

Table 3

Finally, by applying Equation 4.4 we get to the result

$$\left(\frac{d\varepsilon}{d\alpha}\right)_H = 0.290$$

Let's now install the engine on the aircraft model, while keeping the flaps at 0°. By repeating the process shown before, the following plots and values of $C_{M\alpha}$ are obtained:

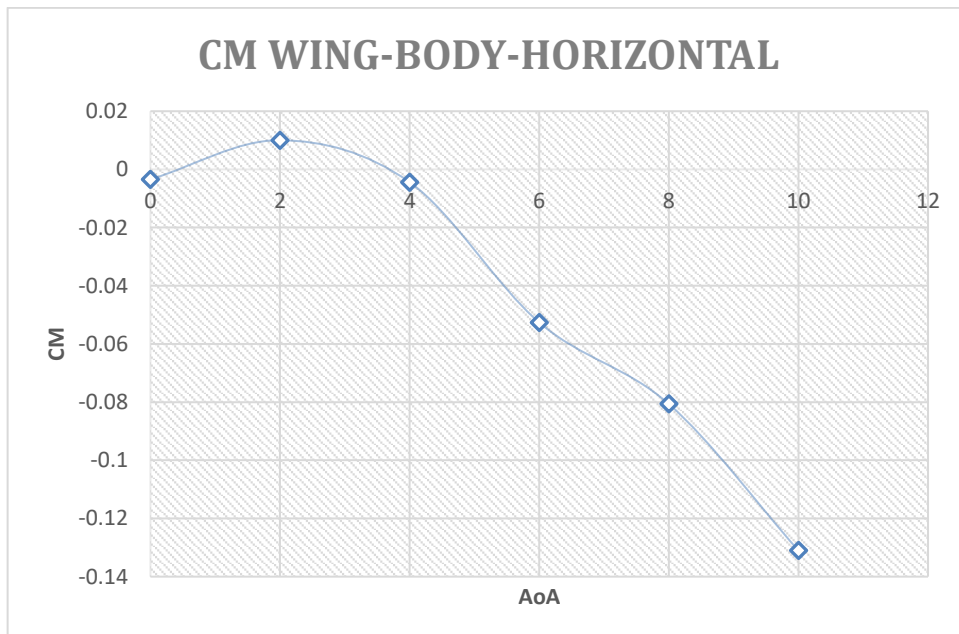


Figure 14 - CM wing-body-horizontal, flaps 0 engines on

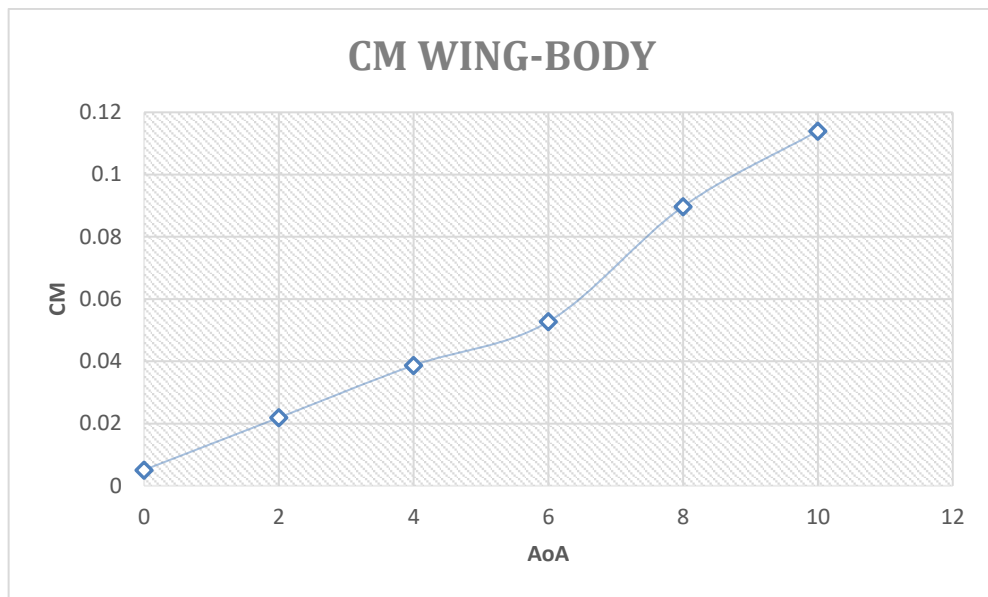


Figure 15 - CM wing-body, flaps 0 engines on

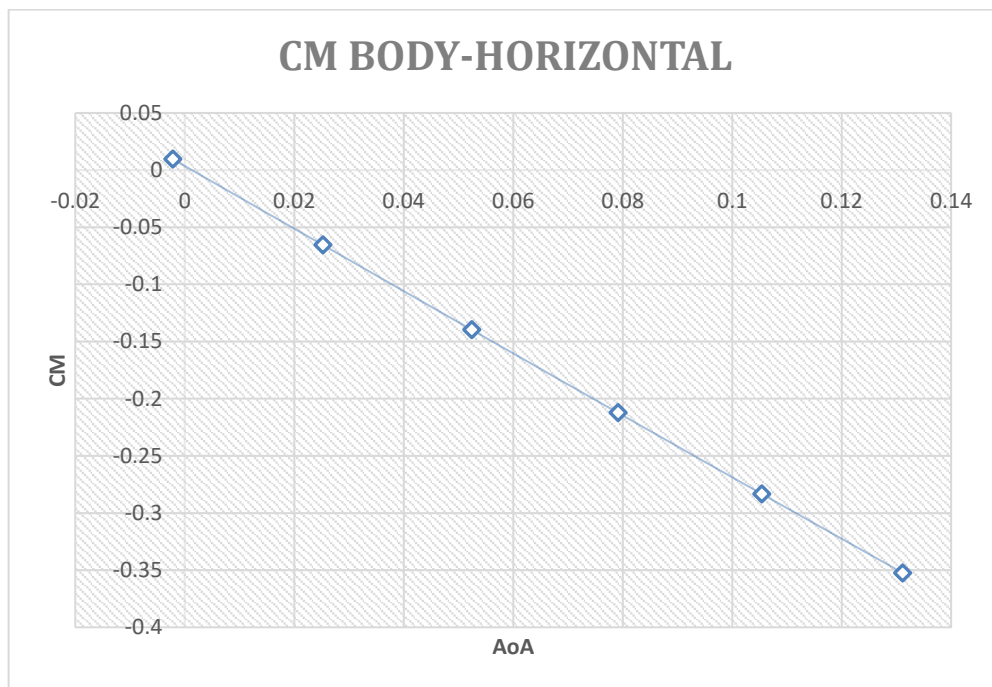
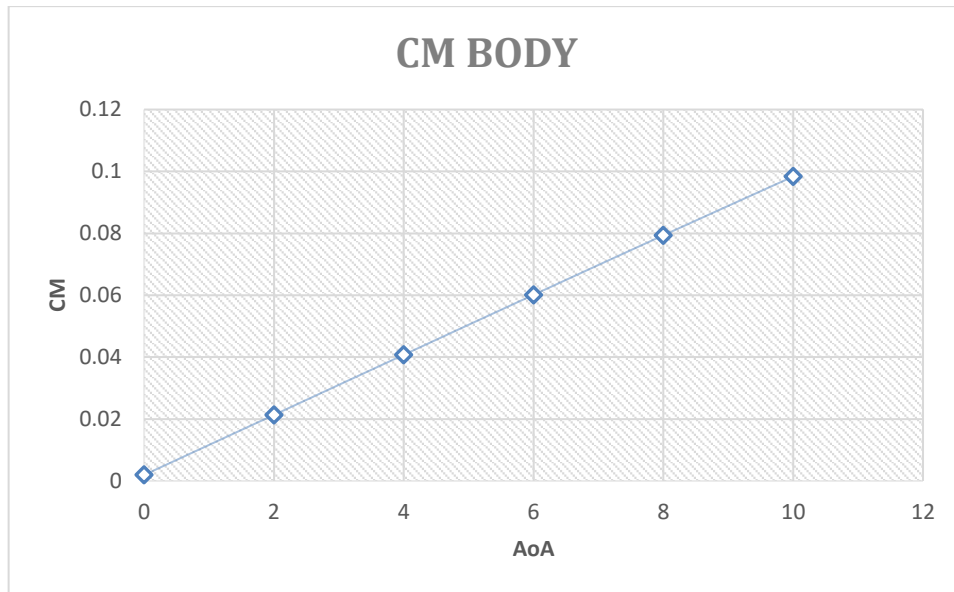


Figure 16 - CM body-horizontal, flaps 0 engines on



As it can be expected, the results don't change in the body-horizontal and body configuration.

Configuration	$C_{M\alpha}$
BWH	-0.014
BW	0.011
BH	-0.036
B	0.010

Table 4

$$\left(\frac{d\varepsilon}{d\alpha}\right)_H = 0.464$$

When deflecting the flaps at 15°, these are the data obtained. Keep in mind that from now on the body-horizontal and body configurations will be neglected, as the deflection of the flaps clearly does not affect those combinations.

Prop – on:

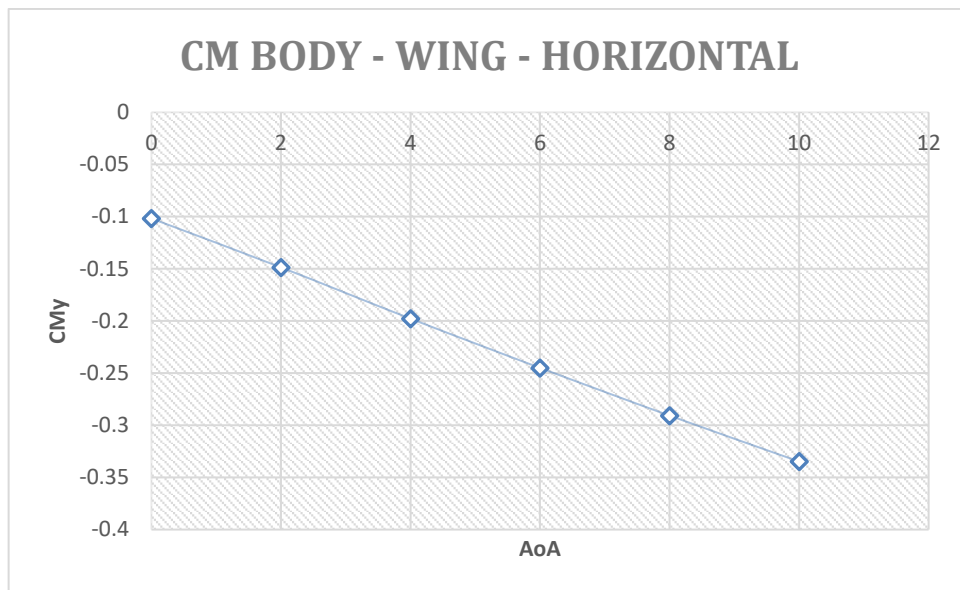


Figure 17 - CM body-wing-horizontal, flaps 15 engines off

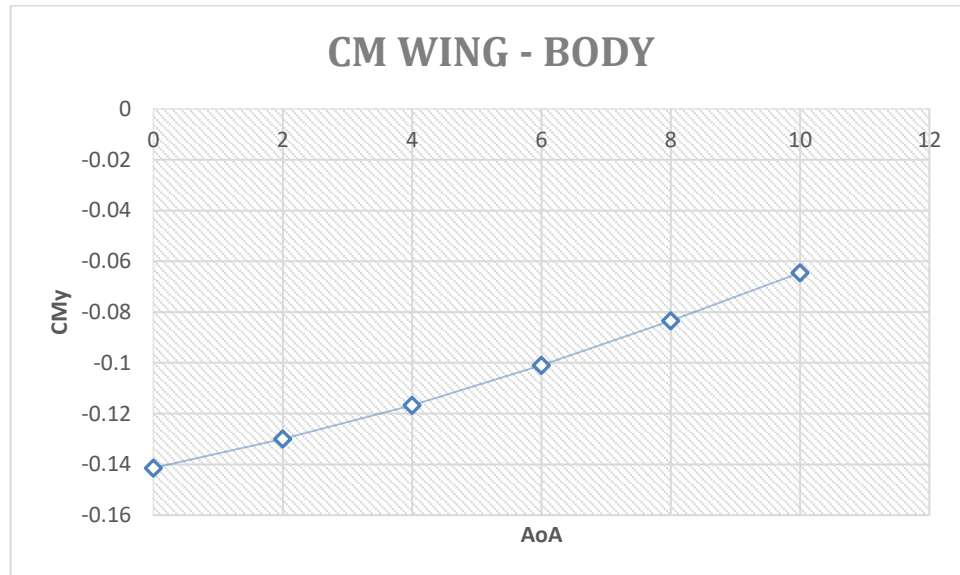


Figure 18 - CM wing-body, flaps 15 engines off

Configuration	$C_{M\alpha}$
<i>BWH</i>	-0.023
BW	0.007

Table 5

$$\left(\frac{d\varepsilon}{d\alpha}\right)_H = 0.322$$

Prop – off:

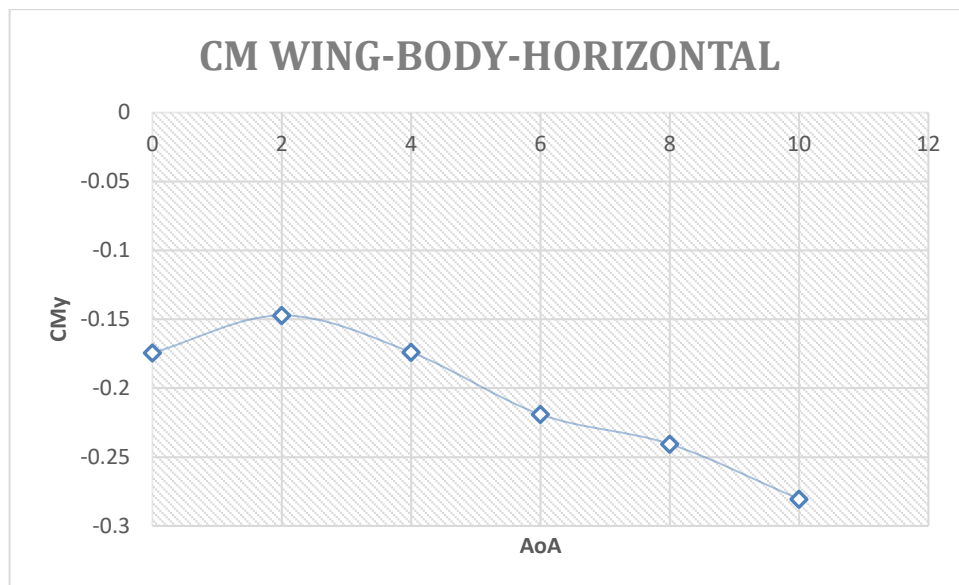


Figure 19 - CM wing-body-horizontal, flaps 15 engines on

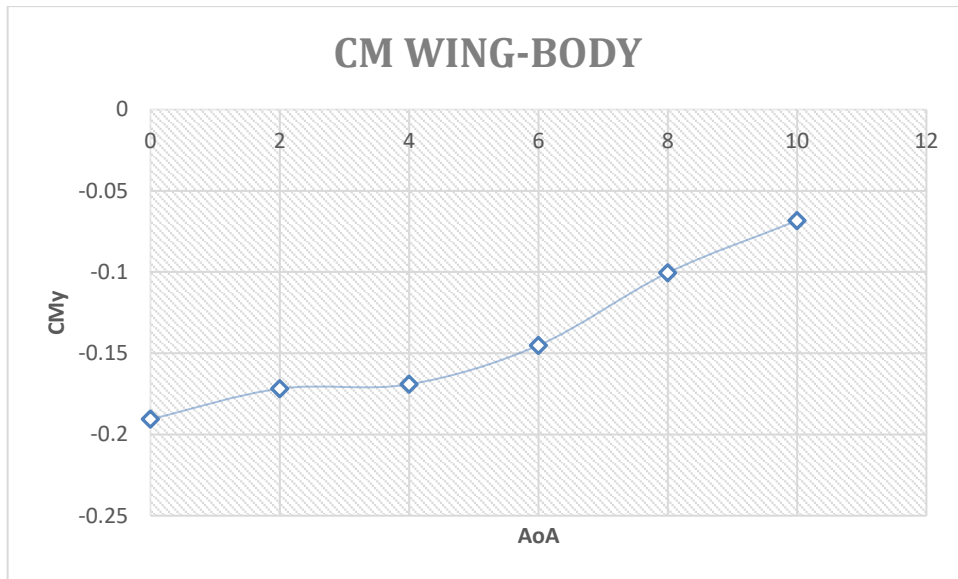


Figure 20 - CM wing-body, flaps 15 engines on

Configuration	$C_{M\alpha}$
<i>BWH</i>	-0.012
BW	0.012

Table 6

$$\left(\frac{d\varepsilon}{d\alpha}\right)_H = 0.469$$

For a 30° flaps deflection:

Prop – off:

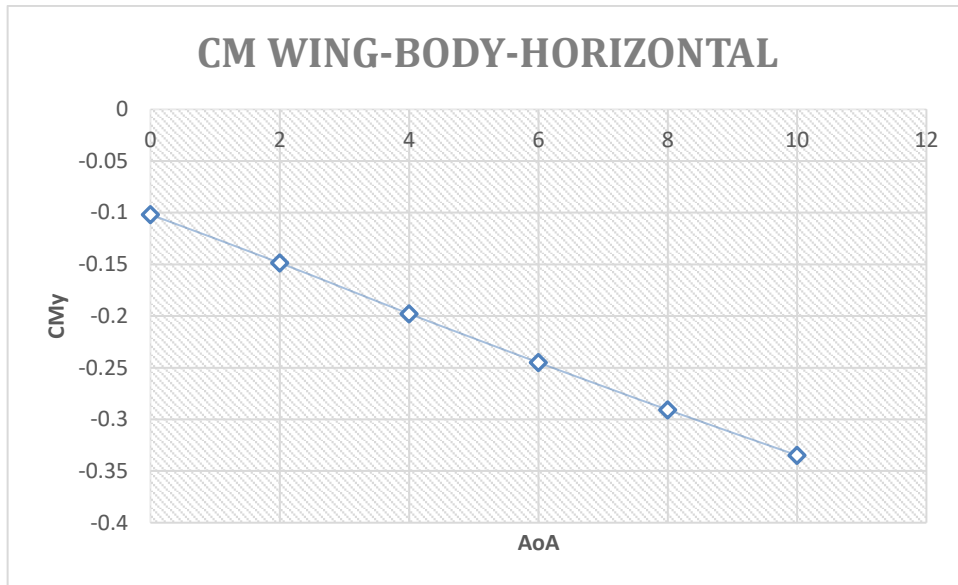


Figure 21 - CM wing-body-horizontal, flaps 30 engines off

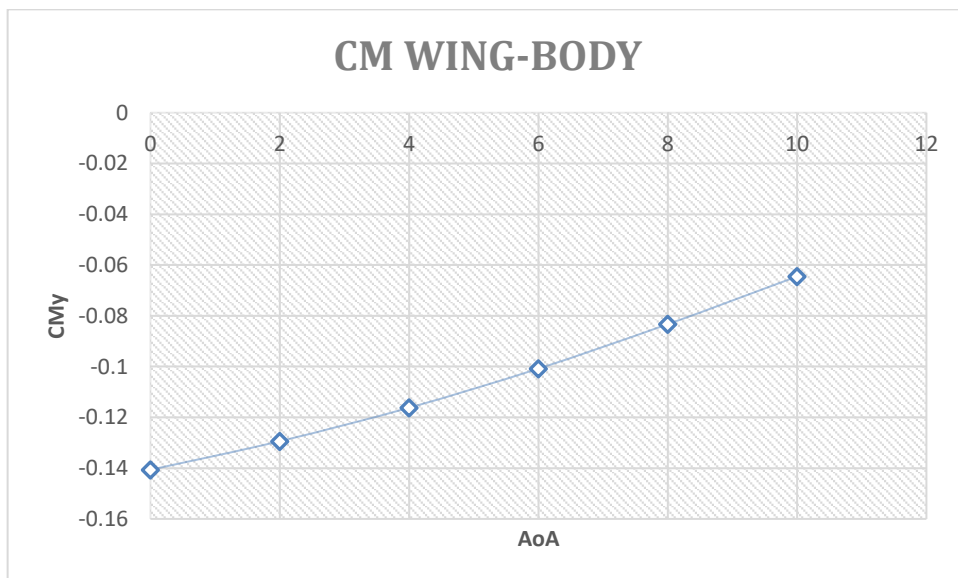


Figure 22 - CM wing-body, flaps 30 engines off

Configuration	$C_{M\alpha}$
<i>BWH</i>	-0.023
BW	0.007

Table 7

$$\left(\frac{d\varepsilon}{d\alpha}\right)_H = 0.323$$

Prop – on:

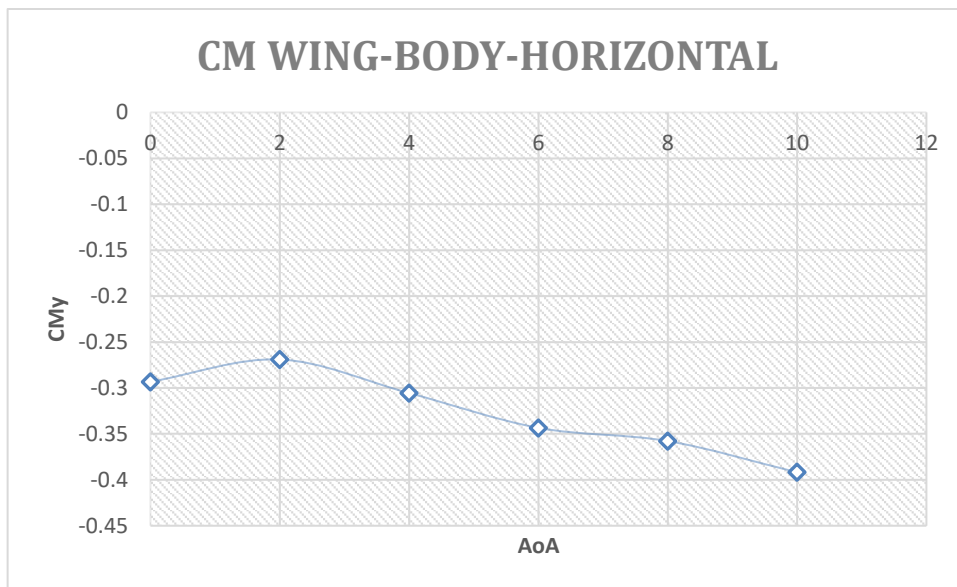


Figure 23 - CM wing-body-horizontal, flaps 30 engines on

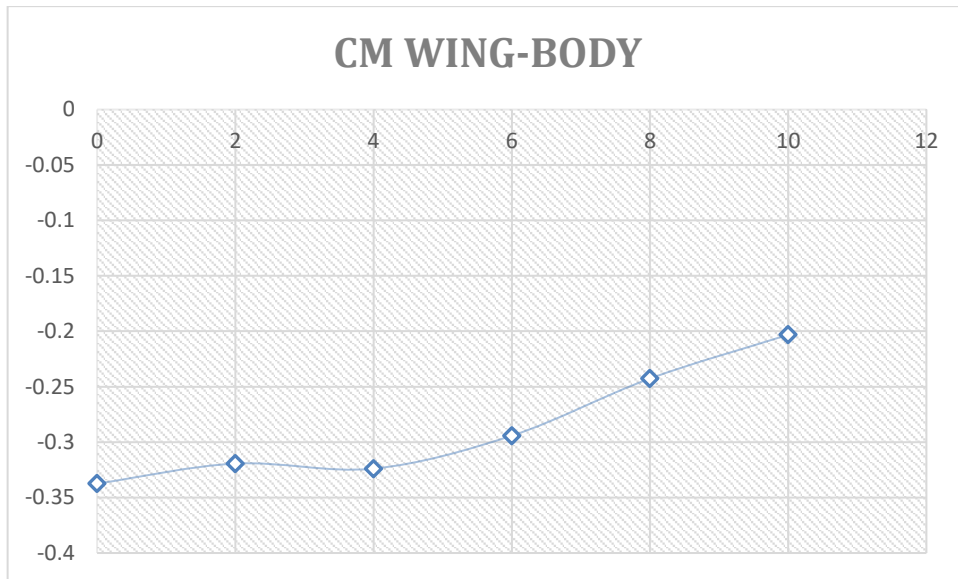


Figure 24 - CM wing-body, flaps 30 engines on

Configuration	$C_{M\alpha}$
<i>BWH</i>	-0.011
BW	0.013

Table 8

$$\left(\frac{d\varepsilon}{d\alpha}\right)_H = 0.462$$

4.2 Method D

This method consists of running the model at first with the horizontal tail removed, obtaining a tail off stability curve, and then with the horizontal tail installed at various angles of incidence (in this case, angles of 0° , -4° , -8° , $+4^\circ$ and $+8^\circ$ will be considered). In the 0° flaps, no propellers configuration, from the polar file we obtain the following table shown in Figure 24:

CM _y TAIL OFF	CM _y 0	CM _y +4	CM _y +8	CM _y -4	CM _y -8	AoA
-0.0485664	0.37171	0.18556	0.01863	0.54115	0.70665	-12
-0.0484926	0.30579	0.11996	-0.04912	0.47727	0.64447	-10
-0.0463973	0.24106	0.05635	-0.11223	0.41414	0.58377	-8
-0.0427969	0.17953	-0.00545	-0.17376	0.35248	0.52354	-6
-0.037522	0.11845	-0.06521	-0.23423	0.29254	0.46692	-4
-0.030374	0.06034	-0.12266	-0.29207	0.23487	0.40695	-2
-0.0216867	0.00326	-0.17846	-0.34831	0.17882	0.35174	0
-0.0113505	-0.05174	-0.2325	-0.40289	0.12408	0.29798	2
0.0006475	-0.10518	-0.28447	-0.45505	0.07097	0.24573	4
0.01424963	-0.15707	-0.33491	-0.50532	0.01905	0.19407	6
0.02938045	-0.20798	-0.38368	-0.55371	-0.03254	0.14295	8
0.04609498	-0.25651	-0.42977	-0.59947	-0.08213	0.0943	10
0.06355425	-0.30516	-0.47518	-0.6451	-0.13197	0.04315	12

Figure 25 - Method C table with VSPAERO data

the combination of all the stability curves is represented in Figure 26

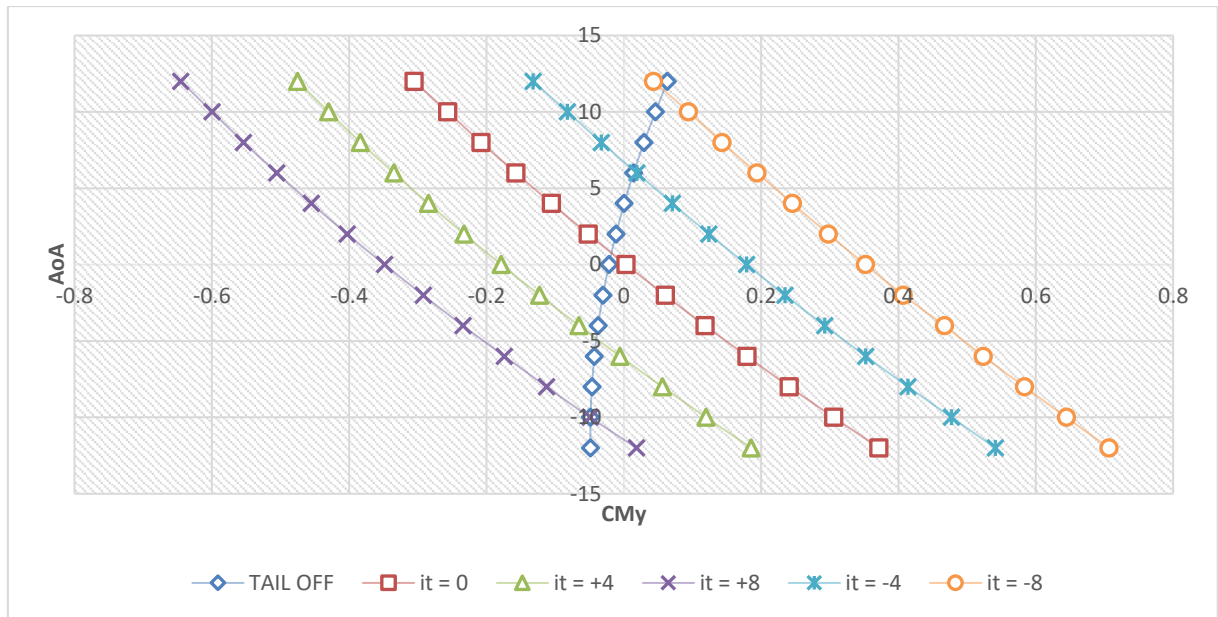


Figure 26 - Stability curves for method D, flaps 0 engines off

The intersections of the tail-off and the tail-on stability curves are points where at a given angle of attack, the tail is at zero lift, therefore:

$$\alpha_t = \alpha_w + i_t - \varepsilon_w = 0 \tag{4.3}$$

Since i_t (angle of incidence) is known and α_w (angle of attack) comes from the points of intersection and therefore can be obtained in MS Excel by using the command shown in Figure 27 it is possible to determine the value of the downwash angle ε_w and to make a plot of ε_w against α_w (Figure 28).

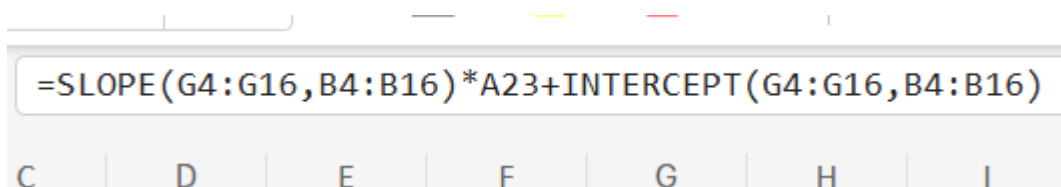


Figure 27 - MS Excel command to find the angle of attack

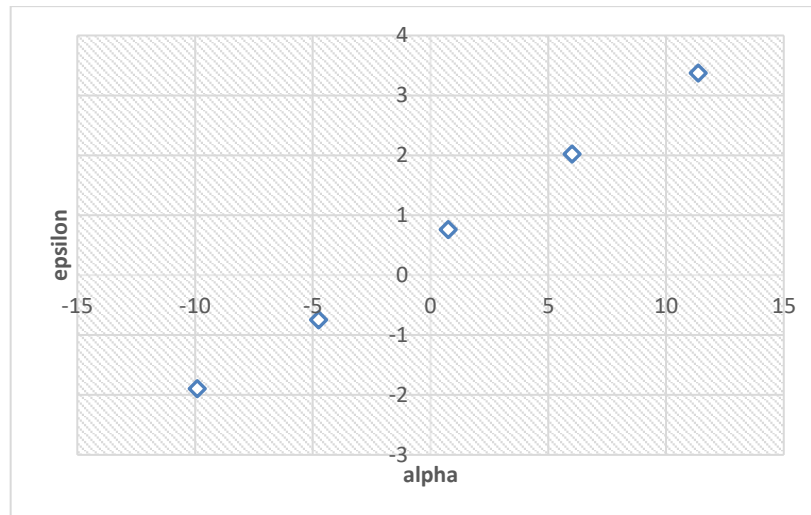


Figure 28 - Epsilon vs alpha

Finally, having defined this curve, a value of the downwash gradient can be obtained by applying once again the excel command SLOPE() :

$$\left(\frac{d\epsilon}{d\alpha}\right)_H = 0.250$$

By applying the same method to the aircraft model with the propellers installed, we get the following plots:

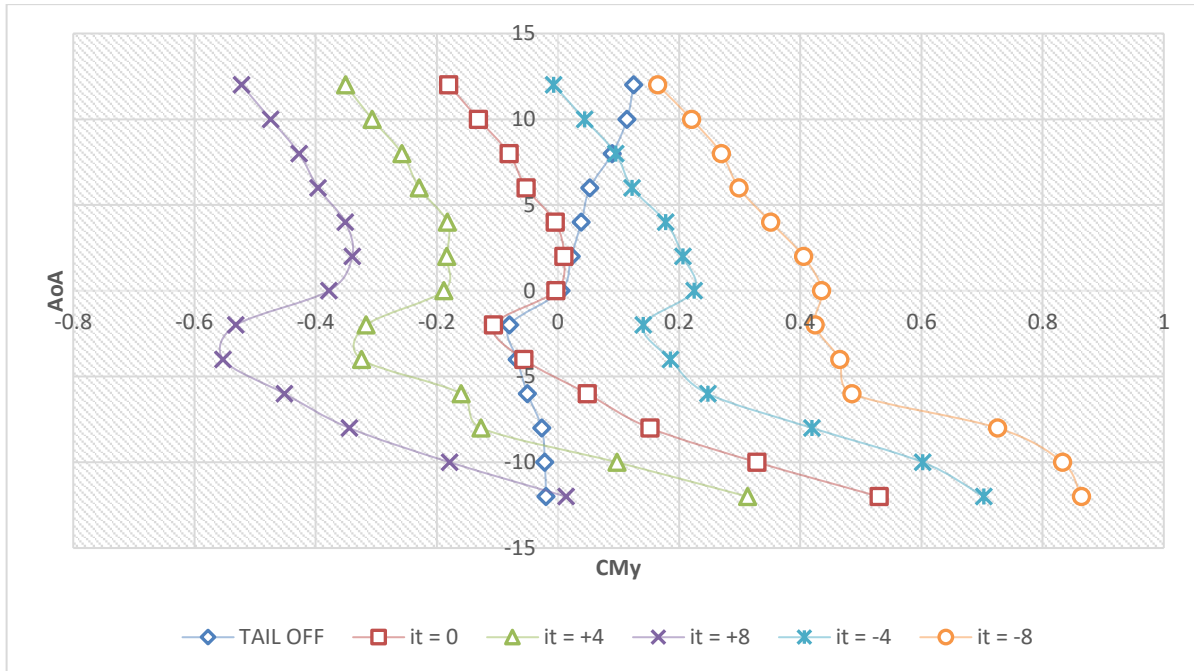


Figure 29 - Stability curves for method D, flaps 0 engines on

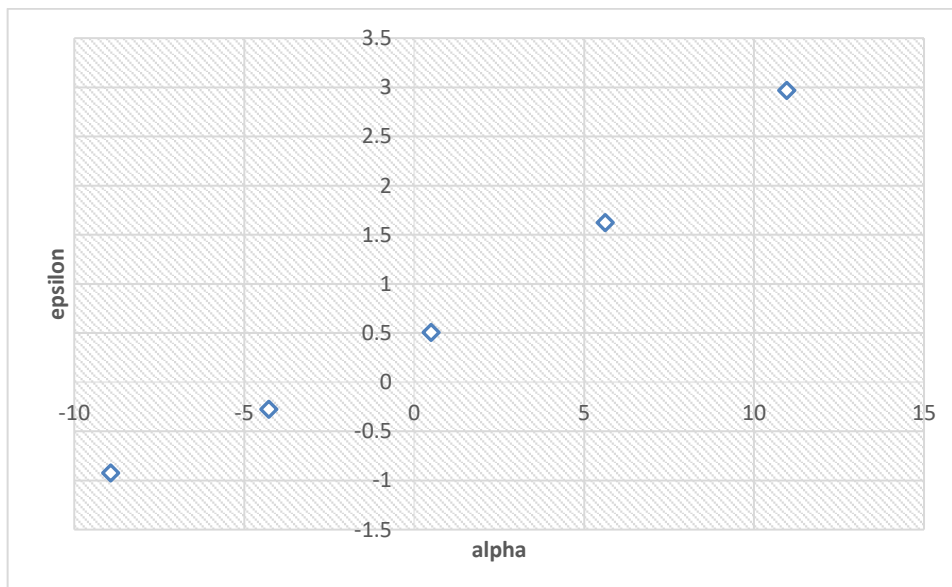


Figure 30 - epsilon vs alpha, flaps 0 engines on

In this case, the downwash gradient assumes a value of

$$\left(\frac{d\varepsilon}{d\alpha}\right)_H = 0.195$$

With the flaps deflected at 15°, the results are the following:

Prop – off:

$$\left(\frac{d\varepsilon}{d\alpha}\right)_H = 0.276$$

Prop – on:

$$\left(\frac{d\varepsilon}{d\alpha}\right)_H = 0.146$$

While, for a 30° flaps deflection, we get

Prop – off:

$$\left(\frac{d\varepsilon}{d\alpha}\right)_H = 0.282$$

Prop – on:

$$\left(\frac{d\varepsilon}{d\alpha}\right)_H = 0.125$$

The results are summarized below in Table 9:

	Prop – off			Prop - on		
	Flaps 0	Flaps 15	Flaps 30	Flaps 0	Flaps 15	Flaps 30
Method A	0.415	<i>not provided by the method</i>				
Method B	0.340	<i>not provided by the method</i>				
Method C	0.290	0.322	0.323	0.464	0.469	0.462
Method D	0.250	0.276	0.282	0.195	0.146	0.125

Table 9

By comparing these results with the ones obtained in a wind tunnel for the model without propellers installed:

Prop – off	
Flaps 0°	0.195
Flaps 15°	0.356
Flaps 30°	0.291

Table 10

5. Conclusion

By looking at Table 9 and Table 10 we can conclude that, as expected, the Prandtl and the USAF DATCOM (methods A and B, respectively) formulas seem to be generally less accurate than the last two methods. Nevertheless, finding an overall best method between method C and D is not as obvious, considering that method C returns a better approximation when the flaps are deflected at 15°, while method D is more accurate with the flaps deflected by 0° and 30°.

Bibliography

- [1] Ciliberti, D.; Buonagura, G; Nicolosi, F.; Longitudinal Wind Tunnel Tests of the PROSIB 19-Pax Airplane. *Appl. Sci.* 2023, 13, 11928.
- [2] Barlow, J. B.; Rae, W. H.; Pope, A. *Low-Speed Wind Tunnel Testing*. 1999.
- [3] Etkin, B.; Rein, D.; *Dynamics of Flight: Stability and Control*. 1995
- [4] <http://openvsp.org>